Sorel Cement Reactions and their Kinetics

Terry A. Ring* and Eric Ping[1]

Chemical Engineering

University of Utah

50 So. Central Campus Drive, MEB 3290

Salt Lake City, UT 84112

---

[1] **Present Address: Chemical Engineering Department, Georgia Institute of Technology, Atlanta, Georgia 30332.**

Abstract

Mixing solid MgO with $MgCl_2$ brine produces Sorel cement. Experimental cement formulations were developed using ratios of 0.898 to 1.318 kg of MgO per liter (7.5 to 11 pounds of MgO per gallon) of brine with brines that vary in $MgCl_2$ concentration from 20% to 33%. X-ray analysis of the set cement after 24 hours indicates that the dominant setting reaction is:

$$5\ MgO + 1\ MgCl_2 + 13\ H_2O \rightarrow 5Mg(OH)_2 \cdot MgCl_2 \cdot 8H_2O\ (\text{5-phase})$$

with a significant amount of material that is amorphous in addition to other minor cement components. Cements formulated near the stoichiometry of the 5-phase reaction, e.g. 0.8987 kg/L (7.5 lbs/gal) and 28.9±0.15% $MgCl_2$ brine, are the strongest. Kinetic experiments observed that the 5-phase is formed quickly, but the kinetics are not complete for several days. The cement does not set by the 5-phase reaction when exposed to Cu Kα x-rays but gives a putty like form having

$MgCl_2$*$6H_2O$ crystals that do not set into a cement. These are the first observations of x-ray altered cementation reaction kinetics.

1. Introduction

Sorel cement is produced by mixing a $MgCl_2$ brine solution with MgO powder. Sorel cement is used as a fast curing cement for patching the surface of freeways as well as other applications including: stucco, flame retardant coatings and molded cement objects. There is considerable controversy in the literature as to what chemical reaction is responsible for the setting reaction of Sorel cement. In the literature [1,2,3] there are several setting reactions presented. The two most prominent are the formation of a 5-phase hydrated magnesium oxychloride product ($5Mg(OH)_2 \cdot MgCl_2 \cdot 8H_2O$) and a 3-phase hydrated magnesium oxychloride product ($3Mg(OH)_2 \cdot MgCl_2 \cdot 8H_2O$) made by the following reactions:

$$5\ MgO + 1\ MgCl_2 + 13\ H_2O \rightarrow 5Mg(OH)_2 \cdot MgCl_2 \cdot 8H_2O \text{ (5-phase)}$$

and

$$3\ MgO + 1\ MgCl_2 + 11\ H_2O \rightarrow 3Mg(OH)_2 \cdot MgCl_2 \cdot 8H_2O \text{ (3-phase)}.$$

Other setting reactions discussed in the literature[4] include the formation of 2-phase ($2Mg(OH)_2 \cdot MgCl_2 \cdot 4H_2O$), 9-phase ($9Mg(OH)_2 \cdot MgCl_2 \cdot 5H_2O$), $Mg(OH)_2$ and $MgCl_2*6H_2O$. In addition to the confusion over the setting reaction, there is a lack of knowledge of the kinetics of the setting reaction and the resulting strength of cements made under different conditions.

This work attempts to first identify which reaction product(s) are observed as a function of the stoichiometry of the mixture, which is adjusted by the ratio of MgO to brine and the brine concentration. Once the reaction products are identified, this work measures the kinetics of the setting reaction using X-ray diffraction analysis. Finally, cement samples with various mixture ratios and brine concentrations are tested for strength. None of the experiments performed use any form of aggregate in the cement mixture, which would tend to increase the strength of the final product.

2. Experimental Materials

Magnesium oxide: MgO used in these experiments came from two sources. One was an ultra pure analytical reagent grade MgO obtained from Sigma® Chemical Company, St. Louis, MO with a purity of 99.999%. The other was an industrial product, MAGOX 98 HR, obtained from Premier Chemicals, LLC of Bettsville, OH. This material is mined as magnesite ($MgCO_3$) in Gabbs, NV and calcined to MgO. A typical chemical analysis for this product is.

Chemical Composition [5]

MgO	85.6% wgt.
CaO	2.7%
SiO_2	2.1%
LOI (H_2O)	4.5%
Fe_2O_3	0.6%
Al_2O_3	0.5%
SO_3	4.0%

The calcium oxide in this material is combined with the free silica as calcium silicate accounting for less than 0.1%. There may also be other trace metals in this material as it is a calcined natural mineral.

<u>$MgCl_2$ brine:</u> Magnesium chloride brine used in these experiments came from two sources. One “pure” brine was prepared from DI water and analytical reagent grade $MgCl_2$*$6H_2O$ crystals with a purity of 99.99% produced by Mallinckrodt Chemical Company, Paris, KY. And the other “impure” brine was obtained from Great Salt Lake Minerals & Chemical Company, (GSLM) Salt Lake City, UT as a by-product of mineral extraction from the Great Salt Lake in Utah. This industrial brine had the following manufacturing specifications.

Chemical Composition[6]

$MgCl_2$	30.00 to 34.00 %wgt.
Sulfate (SO_4^{-2})	0.0 to 3.5%
Potassium (K)	0.0 to 0.7%
Sodium (Na)	0.0 to 0.7%

Water	The balance

However, since this brine is from a natural source it contains other metal cations, inorganic and organic anions.

Water: Water used for dilution of the GSLM brine and for constitution of ”pure” brine and any subsequent dilution was deionized to a conductivity of 18.2 MΩ*cm and filtered to 0.22 microns in a Milli-Q water system[7].

X-ray Standards: For various x-ray standards we used MgO, $Mg(OH)_2$, $MgCl_2*6H_2O$ of analytical reagent grade.

Powder Stabilization: Analytical grade sodium metaphosphate is used at a concentration of 0.1% weight to colloidally stabilize the particles in water solution for particle size measurements.

3. Experimental Methods

Scanning Electron Microscope (SEM) Analysis: Cured cement samples were imaged using a Hitachi S-3000N with energy dispersive x-ray analysis (EDAX) [8]. The cement sample was crushed and a small piece of cement was fixed with carbon tape to the aluminum SEM sample stub. The sample was coated with gold using an RF sputtering apparatus. SEM images were then taken of the cement. In addition, the Premium Chemical Company MgO powder was imaged in the same way and an EDAX analysis was performed on this industrial MgO powder.

Particle Size Distribution: The particle size distribution of the Premium Chemical Company MgO powder was determined using a Beckman Coulter LS230 [9]. A sample of the powder was slurried with DI water using an ultrasonic bath. This sample was further diluted in DI water containing 0.05% sodium metaphosphate in the LS230 to the desired absorbance and analysis performed with the mixing impeller operating at 50%. The sodium metaphosphate is used to colloidally stabilize the particles during the measurement of the particle size distribution.

<u>24 Hour X-ray Analysis:</u> **Cements were prepared by mixing a known amount of MgO with a known amount of brine of a particular $MgCl_2$ concentration. A given weight of the MgO powder was placed in a beaker and 20 mL of the brine of a particular $MgCl_2$ concentration was added and then mixed with a spatula for one minute to ensure the mixture was uniformly mixed. The slurry was allowed to set for a 24 hour period. The sample was then crushed and a powdered sample was loaded into a 1.5 cm x 2.0 cm x 0.2 cm holder. X-ray analysis was performed using a PhillipsX'Pert MPD Diffractometer [10]. All XRD scans were performed with Cu Kα radiation, 45mv/40ma, 0.02° step size, and 0.04 sec/step. Peaks were identified by scanning various standards and consulting the JCPDS-ICDD version 1.2 database. In this database the peaks for 2-phase, 3-phase, 5-phase and 9-phase magnesium oxychloride minerals were given as well as $Mg(OH)_2$ and $MgCl_2*6H_2O$. In addition, the scans performed were analyzed by the PhillipsX'Pert software to identify the various peaks observed in the spectra measured. This software determined the peak heights, backgrounds and peak widths.**

Setting Kinetics: Cements were prepared by mixing a known amount of MgO with a known amount of brine of a particular $MgCl_2$ concentration. The cement paste was placed in the x-ray sample holder (1.5 cm x 2 cm x 2 mm thick) and allowed to set at room temperature. At various time intervals, ranging from soon after the initial mixing of the paste to 24 hours after mixing, the samples were placed in the x-ray beam for analysis. For each spectrum, a new sample was used so that when a sample was scanned, it had no previous x-ray beam exposure.

Strength Tests: Cements were prepared by mixing a known amount of MgO with a know amount of brine of a particular $MgCl_2$ concentration. The mixed paste was placed in a 5.1 cm diameter cylindrical plastic container and allowed to set for 7 days at room temperature. The sample was then removed from the plastic container. The length of the cement cylinder was 7 cm. Strength tests were performed using a Satec Prism 250 press [11] by applying the pressure axially in compression. Five identical samples were prepared and tested. The pressure at

failure for each of the 5 samples was recorded and the average value converted into the compressive stress value at failure and its standard deviation.

MgCl$_2$ concentration: **MgCl$_2$ concentration of the brine obtained from Great Salt Lake Minerals & Chemicals Company (GSLM) was measured with an pHoenix [12] chloride specific ion electrode after dilution 1/1000. Calibration standards were prepared with DI water and MgCl$_2$*6H$_2$O crystals in the 0.1% to 0.5% MgCl$_2$ range. The calibration curve was linear in this region. The concentration measured for our GSLM brine sample showed a concentration of 33.2 ± 0.17% MgCl$_2$ by weight.**

Brine Density: **Brine densities were measured by pyncnometry using a 25±0.02 mL pyncnometer. The pre-weighed pyncnometer was filled with brine and weighed at a temperature of 25±0.5°C. The weight of the brine was measured and the density calculated. These measurements determined a density of 1.290±0.003 gm/cm^3 which is also 32.6±0.26° Baume.**

4. Experimental Results

The MgO from Premier Chemical Company has a particle morphology as shown in Figure 1. Here we see that the powder has a broad particle size distribution and is heavily aggregated. The EDAX analysis shown in Table 1, gives the largest impurities as SiO_2, SO_3 and CaO, which is consistent with the manufacturer's chemical analysis, however, this analysis shows slightly more CaO, SiO_2 and SO_3 and less MgO. The particle size distribution of this MgO powder is given in Figure 2 where 5 replicated scans taken 1 min. apart are plotted. Here we see that the scans are nicely reproducible, indicating that the suspension is colloidally stable. The powder has a broad size distribution with a median size of 16.84 microns. Analysis was performed using a refractive index of 2.24 for the MgO powder [13] and 1.332 for the water [13] at 25±0.5°C.

Cement samples were prepared with pure brine and brine from GSLM and MgO from Premier Chemical Company at various brine concentrations and brine to MgO ratios. There were five

ratios of MgO to brine used as given in Table 2 and three series of these experiments with different brines A) “impure” GSLM brine at 33.2 ± 0.17% $MgCl_2$ by weight, B) “impure” GSLM brine diluted to 28.9±0.15% $MgCl_2$ by weight, C) ”pure” brine at 28.9±0.15% $MgCl_2$ by weight and D) “impure” brine at 20±0.11% $MgCl_2$ by weight. For a reference, the mixture of 0.8987 kg MgO/L (7.5 lbs MgO/gal) with 28.9±0.15% brine, has a slightly higher amount of MgO than a stoichiometric ratio, $MgO:MgCl_2:H_2O$, of 5:1:13 corresponding to the reaction that forms 5-phase. Higher MgO to brine ratios for this brine concentration gives larger amounts of MgO in excess of the 5-phase stoichiometry. The molar ratios for $MgO:MgCl_2:H_2O$ are given in Table 2. Most cements have more MgO than required for the 5-phase reaction. Cements made with 33.2± 0.17% $MgCl_2$ brine and a 0.8987 kg MgO/L (7.5 lb/gal) (MgO to brine ratio) is deficient in MgO and in water. The other ratios in this series of cements, i.e. 0.9586 kg/L (8.0 lb/gal) and higher, have excess MgO in them and are deficient in H_2O for a 5-phase product. These cement mixtures were prepared and allowed to set for 24 hours before x-ray diffraction measurements were made. The x-ray results of these experiments are shown in Figures 3, 7 and 10 for cases A, B and C corresponding to “pure” and “impure” reactants discussed above and in Table 2. At the bottom of each of these figures, the x-ray spectra for pure MgO and “impure” MgO is given, as well as data points that consist of the angle and intensity from JCPDS-ICDD version 1.2 database and specifically measured calibration spectra of pure components of the cement. A comparison of the “pure” and “impure” MgO reveals several impurity peaks at 2θ values of 29˚, 32˚ and 34˚. These impurity peaks correspond to the calcium silicate. These impurity peaks overlap with the peaks associated with $MgCl_2*6H_2O(s)$ which lead to some spectra interpretation problems for the cements in this region of the x-ray spectra.

In Figure 3 the 24 hour x-ray spectra for cements with various MgO to “impure” 33.2 ± 0.17% $MgCl_2$ by weight brine ratios (given in Table 2) are plotted with reference spectra for pure and crude MgO along with data points corresponding to JCPDS-ICDD peak intensities for MgO, $Mg(OH)_2$, $MgCl_2*6H_2O$, 5-phase and 3-phase materials. In all the samples we see that the MgO peak intensity decreases, but not to zero in any of the curves. In addition, many more peaks appear, some of which can be accounted for with the reaction products discussed in the introduction section and others that cannot. The 5-phase reaction product is the dominant reaction product with very little 3-phase, $Mg(OH)_2$ and $MgCl_2*6H_2O$ being produced. The peak heights corresponding to MgO ($2\theta=42.9°$), $Mg(OH)_2$ ($2\theta=58.8°$), $MgCl_2*6H_2O$ ($2\theta=49.8°$), 3-phase ($2\theta=23°$) and 5-phase ($2\theta=11.9°$) observed in Figure 3 are plotted as a function of the ratio of brine to MgO ratio in Figure 4. With increasing amount of MgO to brine, the amount of MgO in the cement increases and the amount of 5-phase decreases slightly after an increase from 0.8987 to 0.9586 kg/L (7.5 to 8 lbs/gal) MgO to brine. This indicates the amount of MgO is not completely reacted and that increasing the MgO to brine ratio leads to even more MgO not consumed by the setting reactions. Figure 5 is a plot of the ratios of peak heights for the 5-phase to MgO and 3-phase to MgO taken from Figure 4. In both cases we see the ratios decrease as the MgO to brine ratio is increased. The ratio of 3-phase to MgO is less than 0.2 for all MgO to brine ratios while the 5-phase to MgO ratio is as high as 0.7 for the 898.7gm/L (7.5 lbs/gal) MgO to brine ratio. If the 5-phase reaction was complete the 5-phase to MgO ratio in the cement should be 0.76.

Figure 6 shows SEM micrographs of the cement A1 after setting for 24 hours. At a magnification of 2,000x, the fracture surface looks somewhat glassy with some features about 8 microns and smaller, an occasional pore ~1 micron in size and the occasional crack as large as 20 microns. At a magnification of 10,000x, the fracture surface shows the cement microstructure to be composed of rounded crystallites with a uniform submicron size. The SEM micrographs for other samples in this A series of cements plotted in Figure 3 are nearly identical to those shown in Figure 6.

The 24 hour x-ray spectra for cements with various MgO to "impure" 28.9±0.15% $MgCl_2$ by weight brine ratios given in Table 2 are plotted in Figure 7 along with reference spectra for pure and crude MgO including data points corresponding to JCPDS-ICDD peak intensities for MgO, $Mg(OH)_2$, $MgCl_2*6H_2O$, 5-phase and 3-phase materials. In all the samples we see that the MgO peak intensity decreases, but not to zero in any of the curves. In addition, many more peaks appear some of which can be accounted for with the reaction products discussed in the introduction section and others that cannot. The 5-phase reaction product is the dominant reaction product with very little 3-phase and $Mg(OH)_2$ being produced. The peak heights corresponding to MgO ($2\theta=42.9°$), $Mg(OH)_2$ ($2\theta=58.8°$), $MgCl_2*6H_2O$ ($2\theta=49.8°$), 3-phase ($2\theta=23°$) and 5-phase ($2\theta=11.9°$) observed in Figure 7 are plotted as a function of the ratio of MgO to brine in Figure 8. With increasing amounts of MgO to brine, the amount of MgO remaining in the cement increases from a non-zero value. The amount of 5-phase decreases with MgO to brine ratio and the amount of 3-phase and $MgCl_2*6H_2O$ are approximately a constant at a low level. Noting that the 0.8987 kg/L (7.5 lbs/gal) of impure 28.9±0.15% $MgCl_2$ brine sample is close to the stoichiometric ratio for a 5-phase cement product, we see that not all the MgO has reacted and that the left over $MgCl_2$ is precipitated as small amounts of 3-phase and $MgCl_2*6H_2O$. Figure 9 shows the ratio of 5-phase to MgO and 3-

phase to MgO as a function of the MgO to brine ratio. The 5-phase to MgO ratio decreases as the MgO to brine ratio increases due to the excess unreacted MgO in the cement. For the 0.8987 kg/L (7.5 lbs per gallon) cement in this series the 5-phase to MgO ratio was 2.6. If the 5-phase reaction was complete the 5-phase to MgO ratio in the cement should be 6.6. The 3-phase to MgO ratio is low and essentially a constant for the different MgO to brine ratios. SEM micrographs of the cements in this B series of cements are essentially identical to those shown in Figure 6. Comparing Figure 8 with Figure 4 we note a similar increase in MgO with MgO to brine ratio, however, the amount of 5-phase is higher with the 28.9±0.15% $MgCl_2$ brine.

In Figure 10, the 24 hour x-ray spectra for cements with various MgO to “pure” 28.9±0.15% $MgCl_2$ by weight brine ratios given in Table 2, are plotted along with reference spectra for pure and crude MgO including the data points corresponding to JCPDS-ICDD peak intensities for MgO, $Mg(OH)_2$, $MgCl_2*6H_2O$, 5-phase and 3-phase materials. In all the samples we see that the MgO peak intensity decreases, but not to zero in any of the curves. In addition many more peaks appear some of which can be accounted for with the reaction products discussed in the introduction section and other small intensity peaks that cannot. The 5-phase reaction product is the dominant reaction product with very little 3-phase, $MgCl_2*6H_2O$ and $Mg(OH)_2$ being produced. The peak heights corresponding to MgO ($2\theta=42.9°$), $Mg(OH)_2$ ($2\theta=58.8°$), $MgCl_2*6H_2O$ ($2\theta=49.8°$), 3-phase ($2\theta=23°$) and 5-phase ($2\theta=11.9°$) observed in Figure 10 are plotted as a function of the ratio of brine to MgO ratio in Figure 11. With increasing ratios of MgO to brine, the amount of MgO remaining in the cement increases and the amount of 5-phase decreases. The amount of $Mg(OH)_2$ and $MgCl_2*6H_2O$ are small and approximately constant with MgO to brine ratio. The amount of 3-phase material first decreases then increases with MgO to brine ratio. Noting that the 0.8987 kg/L (7.5 lbs/gal) of impure 28.9±0.15% $MgCl_2$ brine sample is close to the stoichiometric ratio for a 5-phase cement product we see that not all the MgO has reacted and that the left over $MgCl_2$ is precipitated as small amounts of 3-phase and $MgCl_2*6H_2O$.

Figure 12 shows the ratio of 5-phase to MgO and 3-phase to MgO as a function of the MgO to brine ratio. For the 0.8987 kg/L (7.5 lbs per gallon) cement in this series the 5-phase to MgO ratio was 4.1. If the 5-phase reaction was complete the 5-phase to MgO ratio in the cement should be 6.6. The 5-phase to MgO ratio decreases as the MgO to brine ratio increases due to the excess unreacted MgO in the cement. The 3-phase to MgO ratio initially decreases then remains essentially a constant for the different MgO to brine ratios. SEM micrographs of the cements in this C series of cements are essentially identical to those shown in Figure 6. Comparing Figure 8 with Figure 11, a comparison of brine purity, we see similar trends but the differences lie in the MgO, 5-phase and 3-phase trends with the MgO to brine ratio. Comparing Figure 9 to Figure 12, a comparison of brine purity, the trends are nearly identical. The ratio of 5-phase to MgO is higher with pure brine. The ratio of 3-phase to MgO is not significantly changed by the brine purity.

The change in 5-phase to MgO ratio as a function of MgO to brine ratio for the two "impure" brines, e.g. 33.2±0.17% $MgCl_2$

and 28.9±0.15% $MgCl_2$, is shown in Figure 13. Here we see that the 5-phase to MgO values are much higher with the “impure” 28.9±0.15% $MgCl_2$ brine than with the “impure” 33.2 ± 0.17% brine at low MgO to brine ratios. This suggests that starting with the stoichiometric ratio produces a higher 5-phase to MgO ratio which results in a cement with a high phase purity.

Further analysis of the effect of brine concentration is shown in Figure 14. For this analysis, another diluted “impure” brine was prepared at 20% $MgCl_2$ and used for cement formulation with a MgO to brine ratio of 1.3181 kg/L (11 lbs/gal). With the 20% $MgCl_2$ cements there is a large deficiency of $MgCl_2$ and a large excess of water in the cement formulation. In Figure 14, the 24 hour x-ray spectra for these cements are plotted with reference spectra for pure and crude MgO including data points corresponding to JCPDS-ICDD peak intensities for MgO, $Mg(OH)_2$, $MgCl_2*6H_2O$, 5-phase and 3-phase materials. In all the samples we see that the MgO peak intensity decreases, but not to zero in any of the curves. In addition, many more peaks appear some of which can be accounted for with the reaction products discussed in the introduction section and others that cannot. Figure 15 plots the peak heights for the cement components as a function of brine concentration. The 5-phase reaction product is the dominant reaction product with very little 3-phase, $MgCl_2$*$6H_2O$ and $Mg(OH)_2$ being produced. The MgO peak increases with increasing brine concentration. The cement made with the 20% $MgCl_2$ brine is slow to set and gives a much weaker material by comparison.

The strength of various cement formulations made with “impure” 33.2±0.17% $MgCl_2$ and “impure” 28.9±0.15% $MgCl_2$ brine are shown in Figure 16. The strongest cement with both brines was obtained at 0.8987 kg/L (7.5 lbs/gal) MgO to brine ratio. At higher MgO to brine ratios the compressive strength decreases, but not significantly, until greater than 1.1983 kg/L (10 lbs/gal) MgO to brine ratio. The weakest cement formulation, e.g. 1.3181 kg/L (11 lbs/gal) MgO to brine ratio, was approximately half as strong as the strongest cement formulation. The error bars in Figure 16 are given by the standard deviation of the strength measurement. The error bars are about 20% of the strength measured except in the 1.3181 kg/L (11 lbs/gal) MgO to brine ratio case. These strength measurements were performed without any aggregate of any kind added to them. The addition of aggregate will further increase the compressive strengths of the cements.

5. Kinetics of Cementation Reaction

In our initial attempts to determine the kinetics of the setting reaction, we prepared a single A1 cement sample with 0.8987 kg/L (7.5 lbs/gal) of "crude" MgO in 33.2±0.17% "impure" $MgCl_2$ brine and placed it in the x-ray spectrometer taking one scan after another for 24 hours. The results were surprising in that the cement did not set at 24 hours as it had done without x-ray exposure. Instead, a putty like material resulted after 24 hours with x-ray exposure instead of a solid cement without x-ray exposure. A second attempt with both A1 and A4 cements gave the same result – x-ray exposure prevented the completion of the setting reaction. The x-ray spectra for the A1 sample both with and without continuous x-ray exposure after 24 hours is shown in Figure 17. With x-ray exposure, a large amount of $MgCl_2*6H_2O$ is observed and very little 5-phase is observed. This is in stark contrast to the results without x-ray exposure where the 5 phase is predominately observed. As a result, we can definitively state that Cu K_α x-ray exposure prevents the 5-phase reaction and promotes the production of $MgCl_2*6H_2O$. This is rather surprising result. After an extensive literature search, we were not able to find any other reports that show that x-ray radiation can alter the course of cementation reactions of any type. Polarized laser light radiation [15] and a strong DC electric field [16], however, have been shown to alter the crystal polymorph during crystallization. Since in its most general form cementation is simply a dissolution reaction followed by a crystallization reaction, these experimental results using x-ray radiation are likely to be part of a more common theme of radiation altered crystallizations.

As a result, the protocol to measure cementation kinetics had to be changed. A series of cement samples were prepared with the same ingredients as A1 in Table 2 and after a given period of time one of the samples was placed in the x-ray spectrometer for analysis. The sample was only exposed to the x-ray beam once and then discarded. The results of these experiments were analyzed for spectral peaks and the peaks corresponding to MgO and 5-phase are plotted as function of setting time in Figures 18 and 19, respectively. Here we see that as setting time increases the amount of 5-phase increases and the amount of MgO decreases then increases. The MgO behavior is not expected. We would expect a uniform decrease in MgO, however, a closer look at the x-ray spectrum in the early times of setting shows that there is a large broadening of the spectrum from 2θ of 20° to 60°, see Figure 20. This is due to a fraction of the cement material being poorly crystallized or amorphous material that with time becomes more crystalline. This broadening is most pronounced for times less than 60 min. Then it lessens. Due to this broadening, the peak height, which is calculated by taking the peak height and subtracting the local baseline, is thereby decreased and as a result, the MgO trace in Figure 19 decreases then increases due to these amorphous phases present at short times.

6. Conclusions

Cements made from MgO and $MgCl_2$ brines set predominately by the reaction:

$5\ MgO + 1\ MgCl_2 + 13\ H_2O \rightarrow 5Mg(OH)_2 \cdot MgCl_2 \cdot 8H_2O$ (5-phase**).**

The setting time is in less than 4 hrs, however, the setting reaction continues for up to 72 hours at an ever-slower rate. After 24 hours of setting, the cements have substantial strengths. Cements with ratios that are stoichiometric with the 5-phase reaction are the strongest observed.

X-ray exposure during setting alters the course of the 5-phase setting reaction giving $MgCl_2*6H_2O$ instead. X-ray expose during setting yields a putty-like material and not hardened cement.

7. Tables

Table 1. EDAX analysis of Premium Chemical MgO Powder

Element	Weight %	Mole %
MgO	84.47	89.28
SiO_2	3.98	2.82
SO_3	3.84	2.04
CaO	7.71	5.95
Total	100.00	100.00

Table 2. MgO to Brine Ratios used for XRD and Strength Experiments. All cements contain the Premium Chemical MgO Powder as a source of MgO.

Code	Brine % wgt. $MgCl_2$	lbs/gal	kg/L	Molar Ratio $MgO:MgCl_2:H_2O$
A1	33.2 ± 0.17	7.50	0.89874	4.96:1:10.64
A2	33.2 ± 0.17	8.00	0.95865	5.29:1:10.64
A3	33.2 ± 0.17	9.00	1.07845	5.95:1:10.64
A4	33.2 ± 0.17	10.00	1.1983	6.61:1:10.64
A5	33.2 ± 0.17	11.00	1.3181	7.27:1:10.64
B1	28.9 ± 0.15	7.50	0.89874	5.75:1:13
B2	28.9 ± 0.15	8.00	0.95865	6.13:1:13
B3	28.9 ± 0.15	9.00	1.07845	6.90:1:13
B4	28.9 ± 0.15	10.00	1.1983	7.66:1:13
B5	28.9 ± 0.15	11.00	1.3181	8.43:1:13
C1	28.9 ± 0.15	7.50	0.89874	5.75:1:13
C2	28.9 ± 0.15	8.00	0.95865	6.13:1:13
C3	28.9 ± 0.15	9.00	1.07845	6.90:1:13
C4	28.9 ± 0.15	10.00	1.1983	7.66:1:13
C5	28.9 ± 0.15	11.00	1.3181	8.43:1:13
D5	20 ± 0.11	11.00	1.3181	13.31:1:21.14

Brines used

A Series - “impure” GSLM brine at 33.2 ± 0.17% weight $MgCl_2$

B Series - “impure” GSLM brine diluted to 28.9±0.15%wgt $MgCl_2$

C Series - ”pure” brine at 28.9±0.15%wgt $MgCl_2$

D Series - “impure” GSLM brine diluted to 20±0.11%wgt $MgCl_2$.

8. <u>Figures</u>

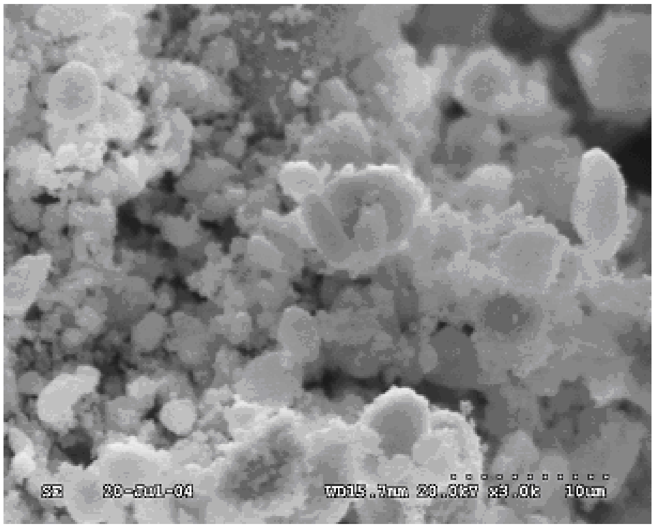

Figure 1. SEM of Premier Chemicals MgO Powder at 3000x Magnification. Dotted Bar = 10 microns.

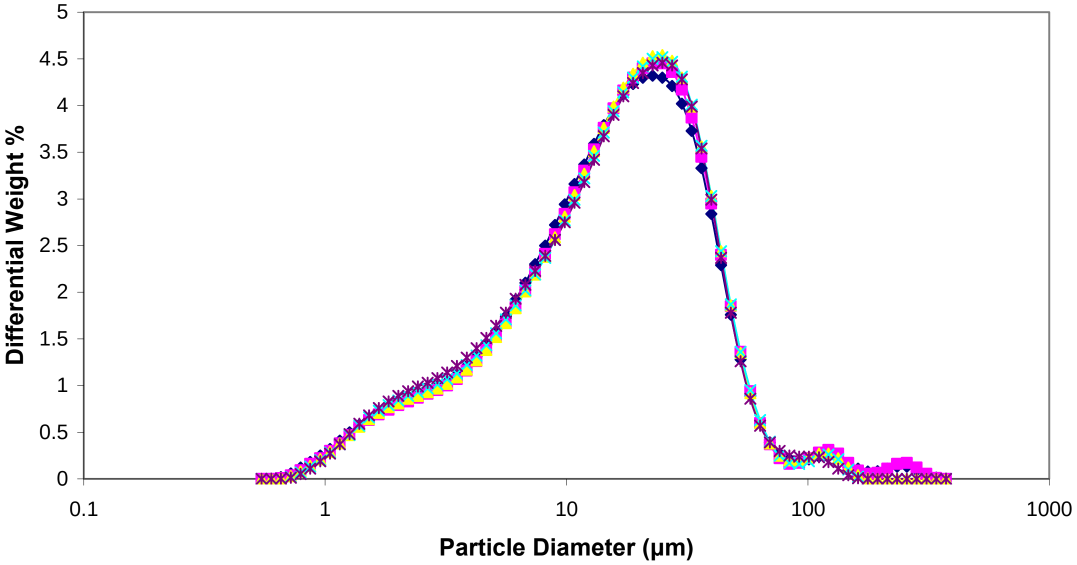

Figure 2. Particle Size Distribution (Differential Volume vs. diameter) of Premier Chemicals MgO Powder using Beckmann Coulter LS230. The various traces correspond to replicate analysis taken at 1-minute interval. Some small amount of aggregation is observed with the latter samples.

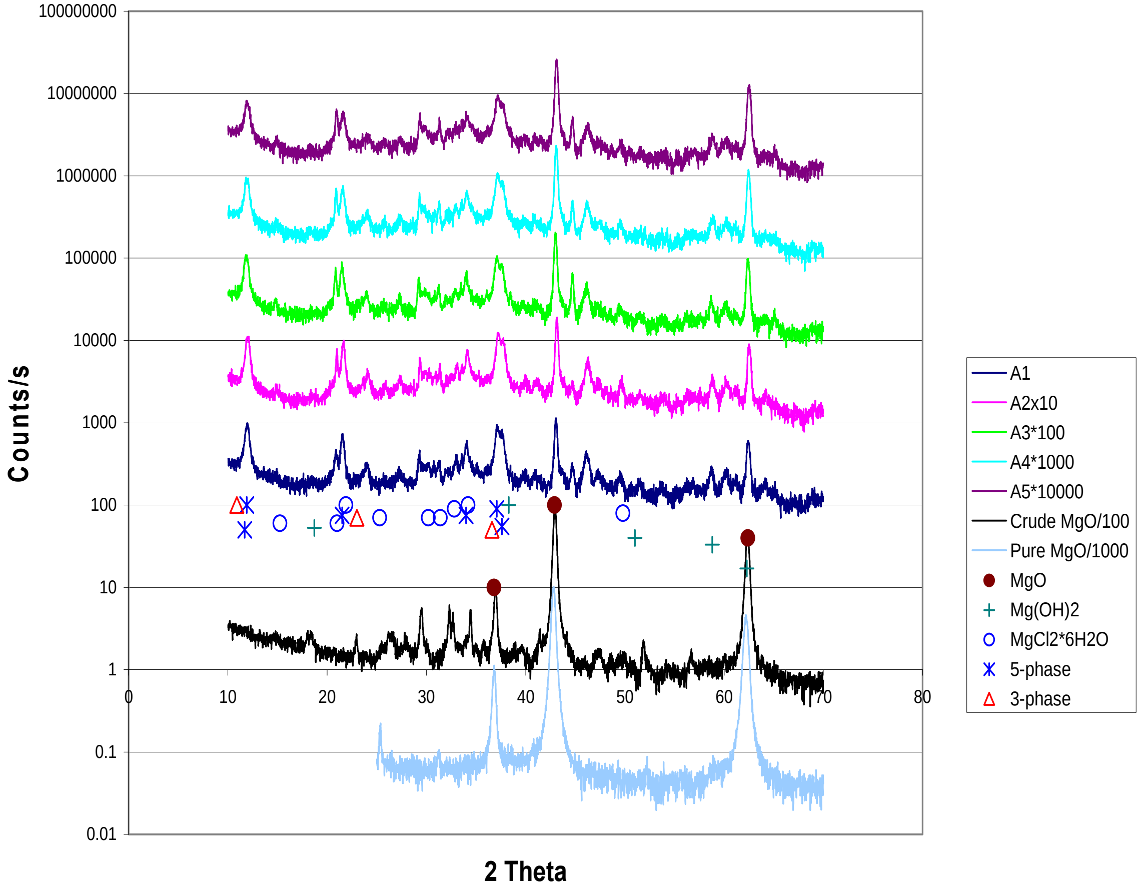

Figure 3. X-ray diffraction analyses of cements allowed to set for 24 hours. These A series cements were made with various MgO to "impure" 33.2 ± 0.17% $MgCl_2$ by weight brine ratios given in Table 2. Data points indicate the location and intensity of peaks according to JCPDS-ICDD.

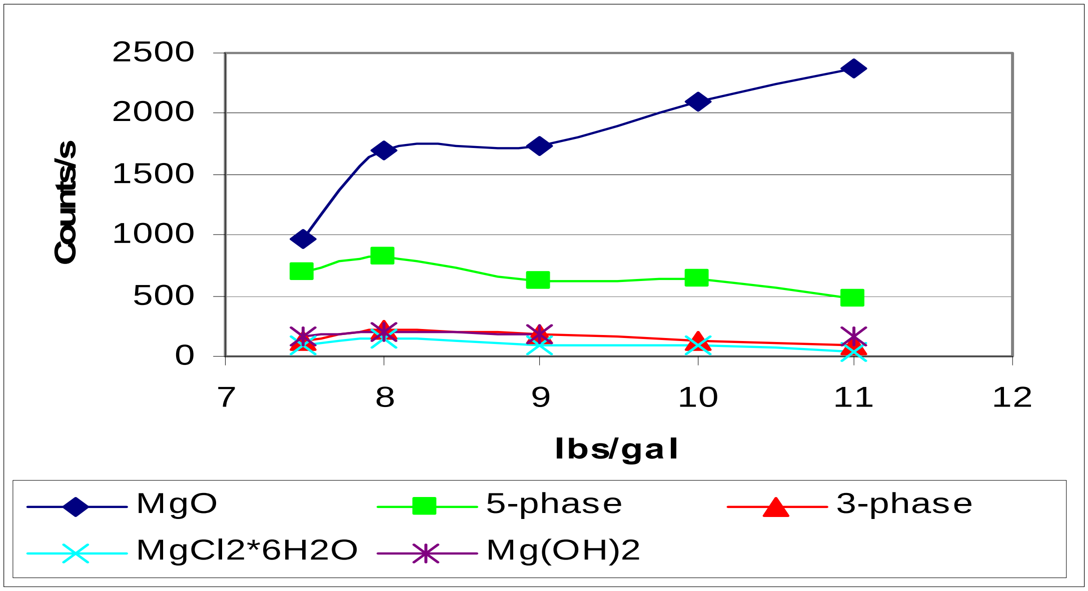

Figure 4. Plot of 24 hour x-ray peak heights corresponding to MgO (2θ=42.9°), 3-phase (2θ=23°) and 5-phase (2θ=11.9°) observed in Figure 3 are plotted as a function of the "impure" 33.2 ± 0.17% $MgCl_2$ brine to MgO ratio.

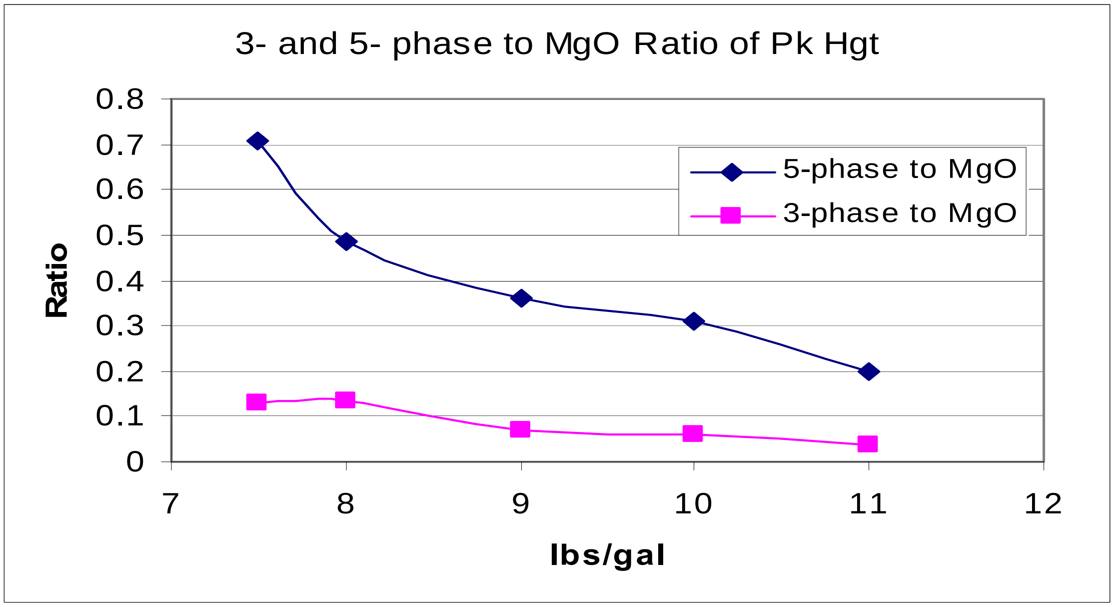

Figure 5. Plot of the ratio of 24-hour x-ray peak heights corresponding to the 5-phase to MgO ratio and the 3-phase to MgO ratio observed in Figure 3 are plotted as a function of the "impure" 33.2 ± 0.17% $MgCl_2$ brine to MgO ratio.

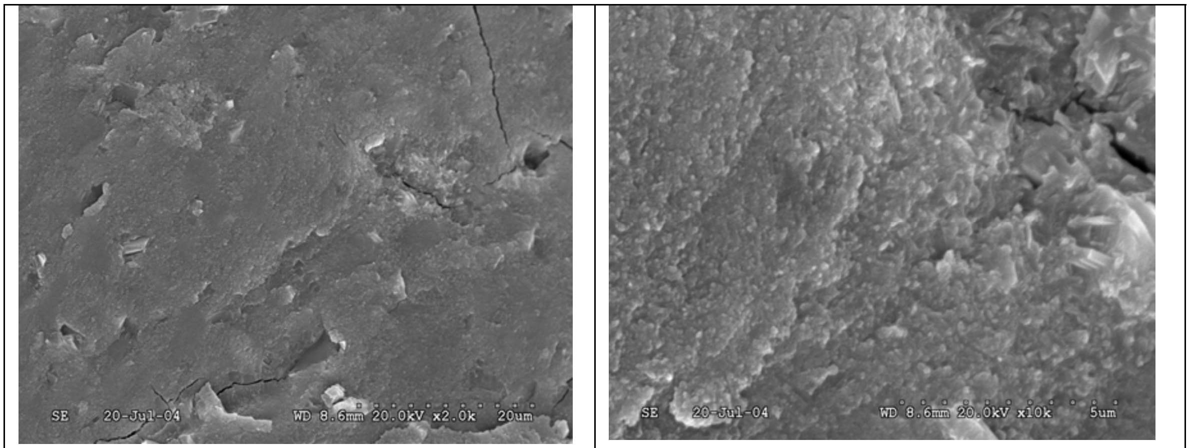

Figure 6. Scanning Electron Micrograph of cement A1 at two magnifications; 2,000x (dotted bar = 20 microns) and 10,000x (dotted bar = 5 microns).

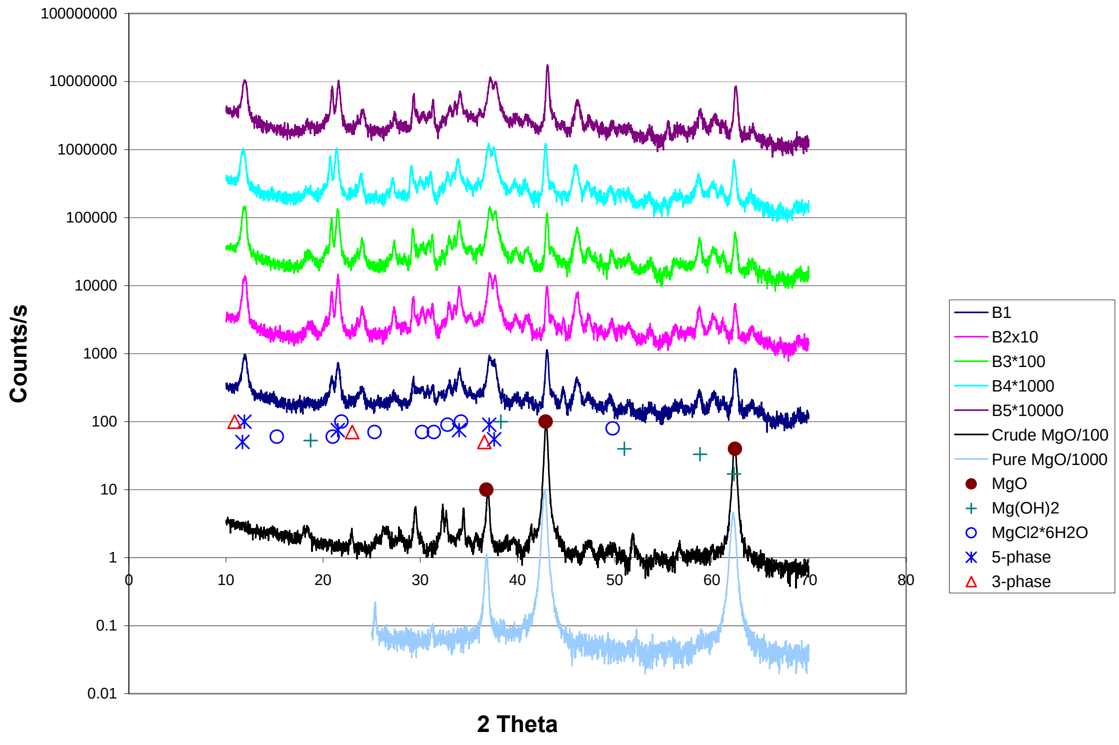

Figure 7. X-ray diffraction analyses of cements allowed to set for 24 hrs. These B series cements were made with various MgO to "impure" 28.9±0.15% $MgCl_2$ by weight brine ratios given in Table 2. Data points indicate the location and intensity of peaks according to JCPDS-ICDD.

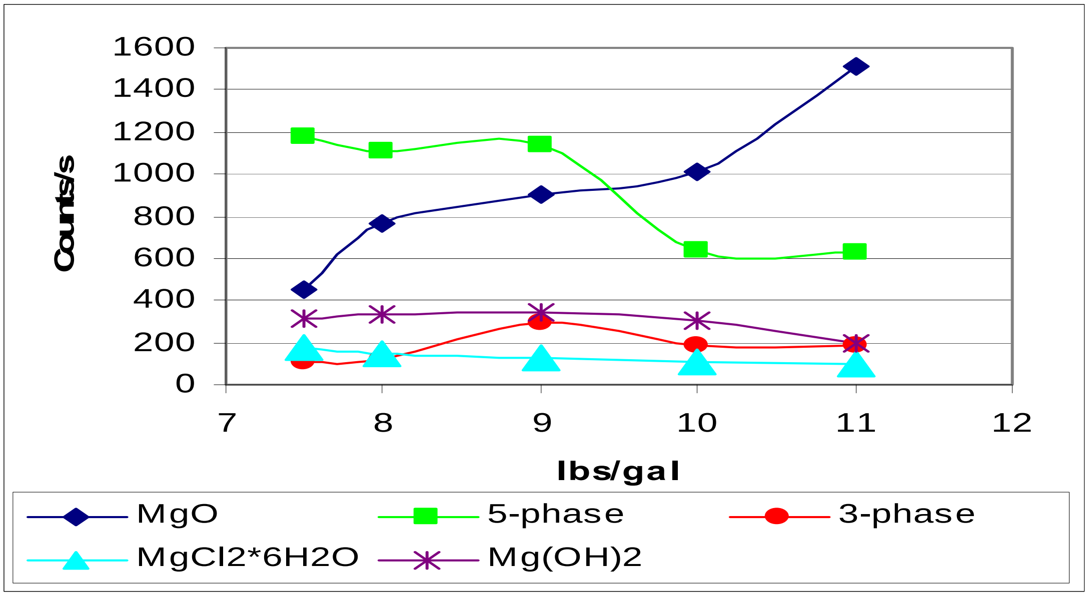

Figure 8. 24 hour x-ray diffraction peak heights from Figure 7 versus MgO to cement ratio for impure 28.9±0.15% weight $MgCl_2$ Brine and impure MgO.

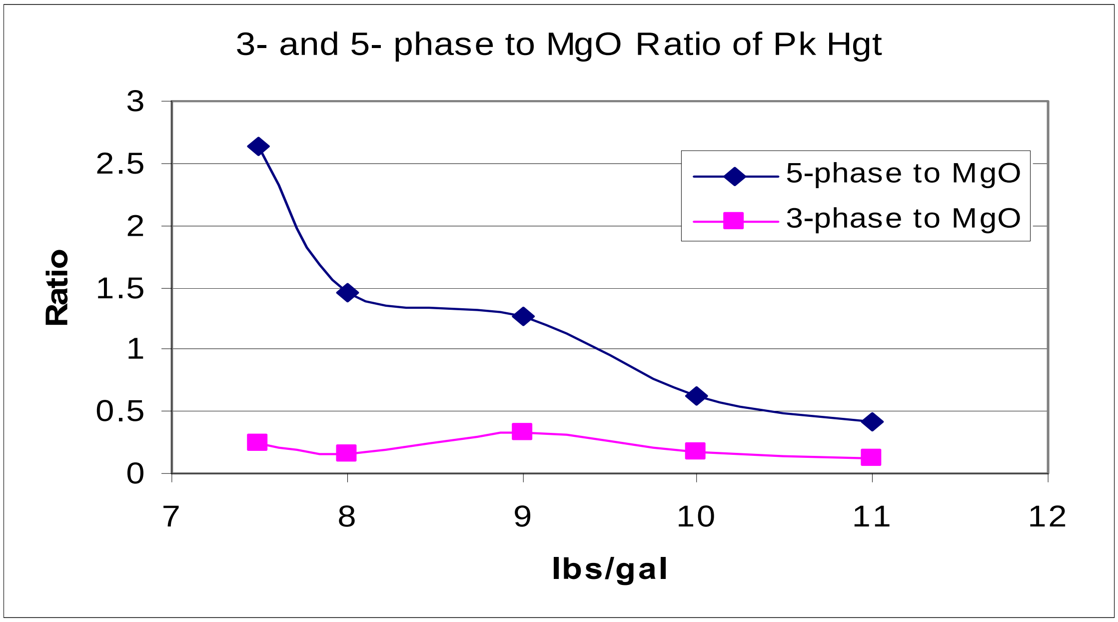

Figure 9. **Plot of the ratio of 24 hour x-ray peak heights corresponding to the 5-phase to MgO ratio and the 3-phase to MgO ratio observed in Figure 7 are plotted as a function of the "impure" 28.9±0.15% $MgCl_2$ brine to MgO ratio.**

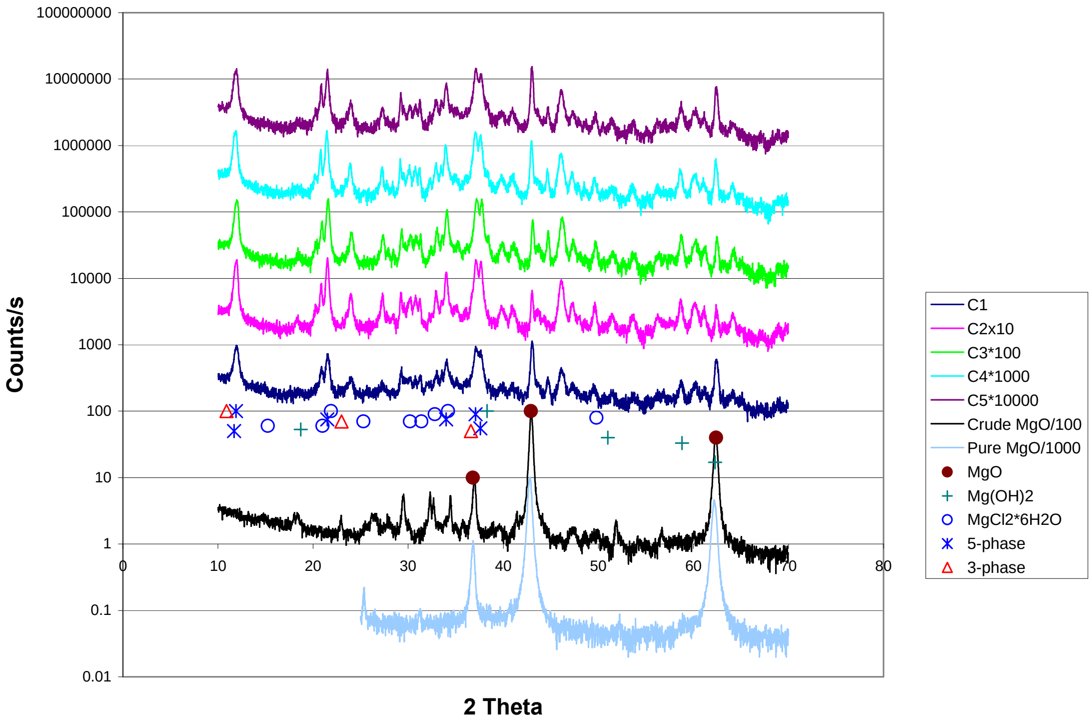

Figure 10. X-ray Diffraction analyses of cements allowed to set for 24 hours. These C series cements were made with various MgO to "pure" 28.9±0.15% $MgCl_2$ by weight brine ratios given in Table 2. Data points indicate the location and intensity of peaks according to JCPDS-ICDD.

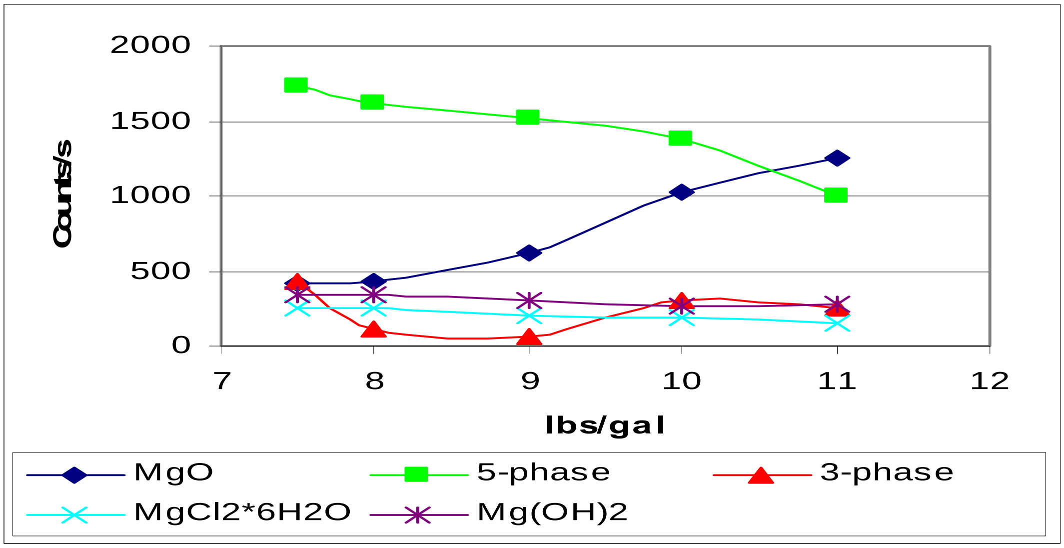

Figure 11. 24 hour x-ray diffraction peak heights from Figure 7 versus MgO to cement ratio for "pure" 28.9±0.15% weight $MgCl_2$ Brine and impure MgO.

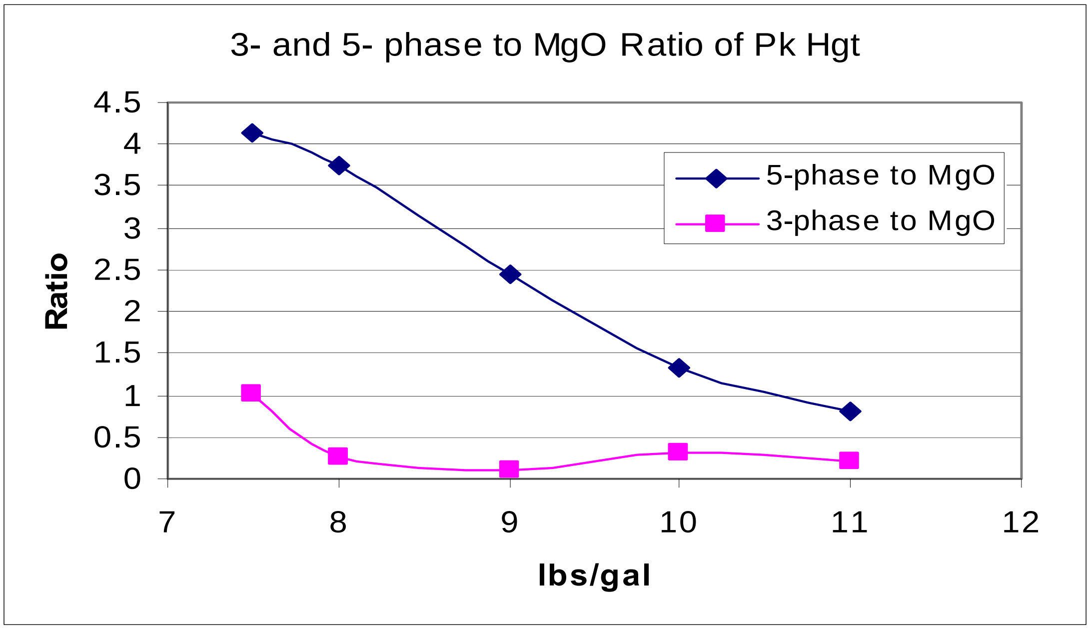

Figure 12. Plot of the ratio of 24 hour x-ray peak heights corresponding to the 5-phase to MgO ratio and the 3-phase to MgO ratio observed in Figure 7 are plotted as a function of the "pure" 28.9±0.15% $MgCl_2$ brine to MgO ratio.

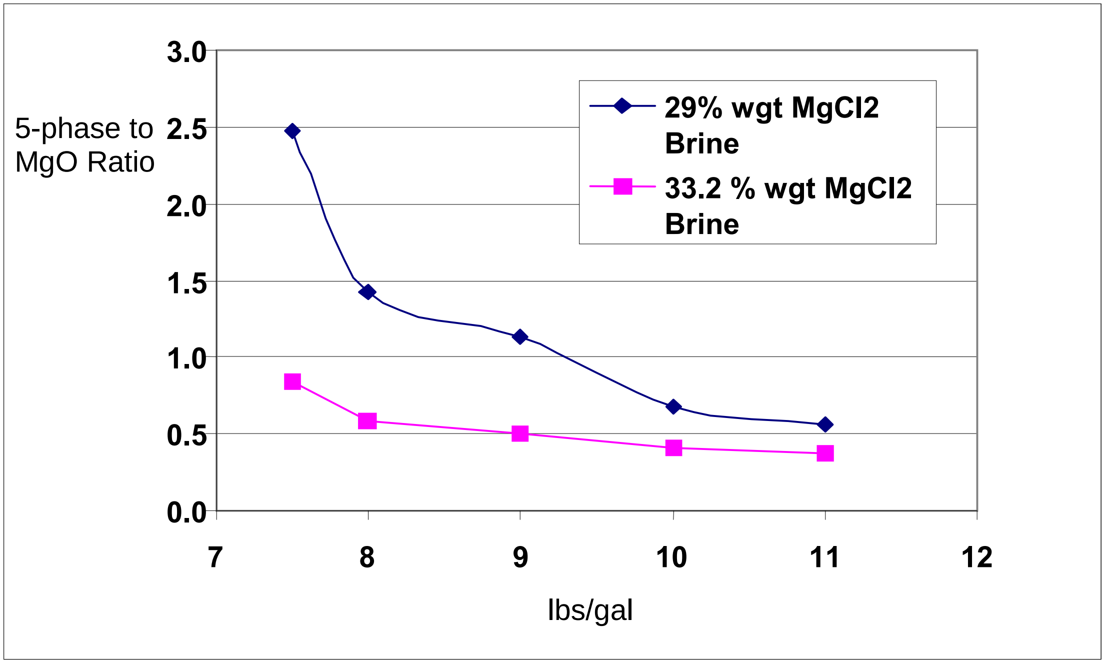

Figure 13. Ratio of XRD peak heights for 5-phase to MgO in cements set for 24 hours with different ratios of MgO to brine. In both cases the brine is "impure" GSLM brine.

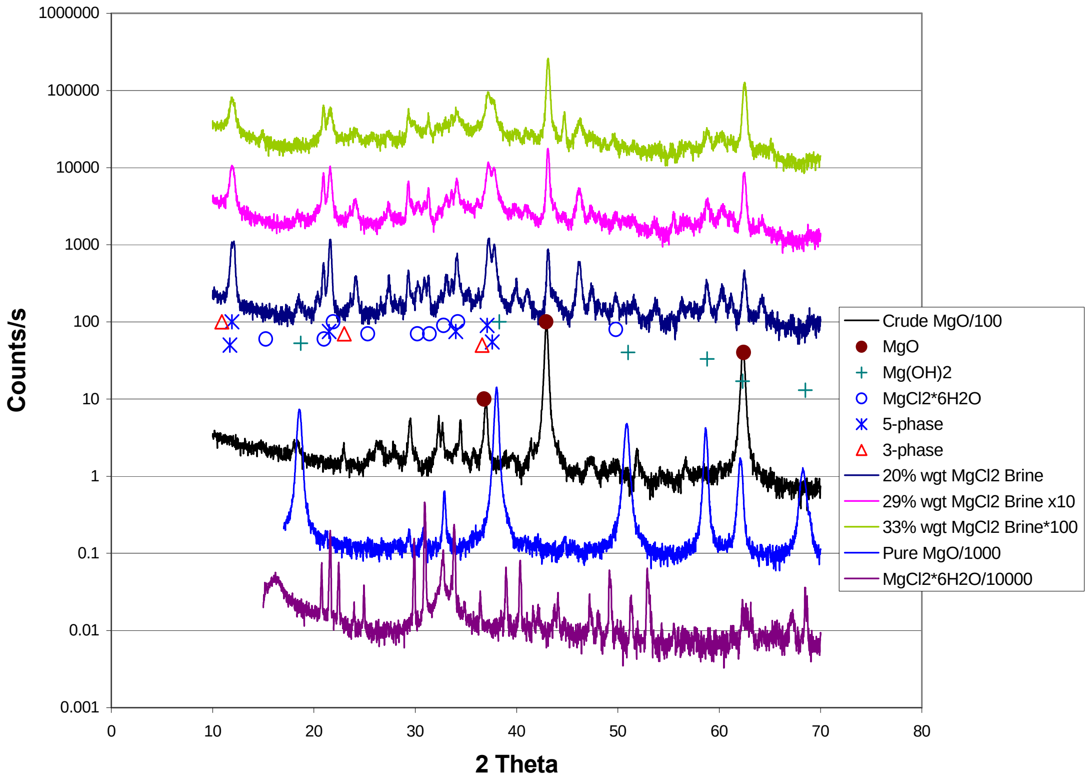

Figure 14 X-ray diffraction data for cement samples allowed to set for 24 hours made with different Brine concentrations and1.3181 kg/L (11 lbs MgO/gal).

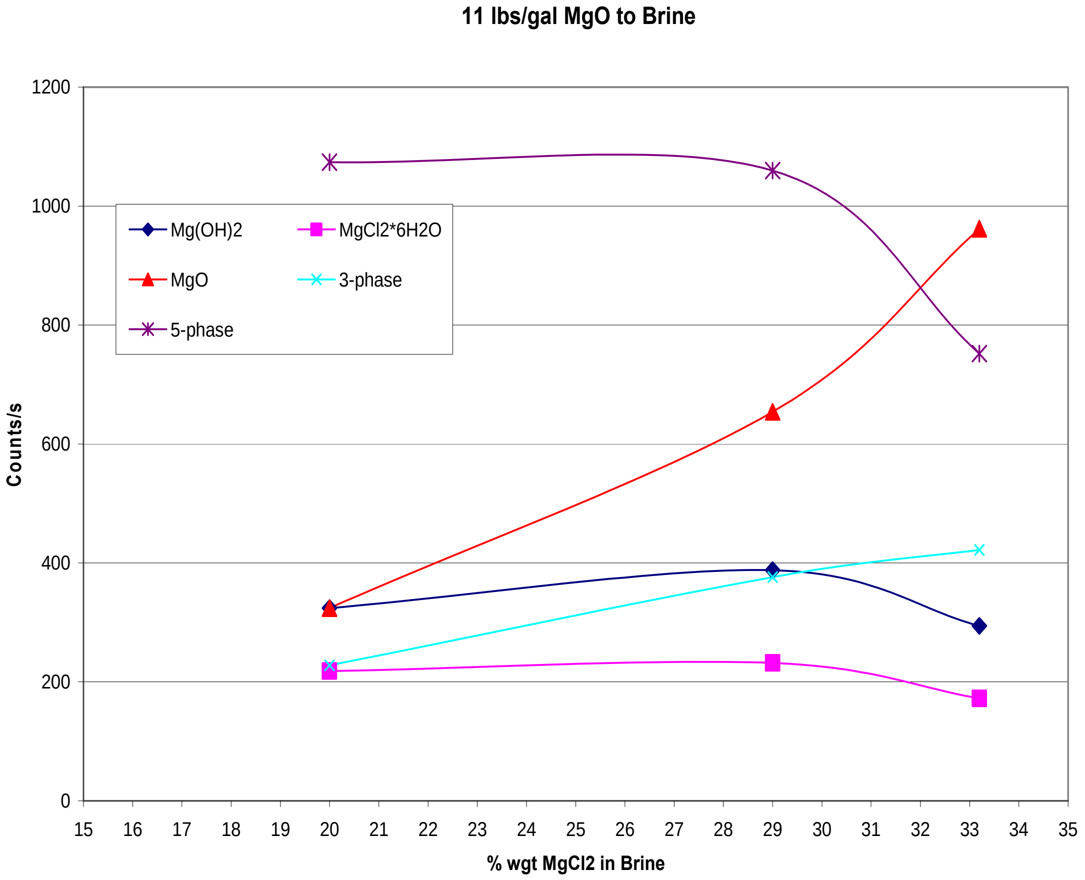

Figure 15. 24 hour x-ray diffraction peak heights from Figure 14 versus "impure" $MgCl_2$ brine concentration from 20 to 33 % $MgCl_2$ for cements made with 1.3181 kg/L (11 lbs/gal) impure MgO to brine ratio.

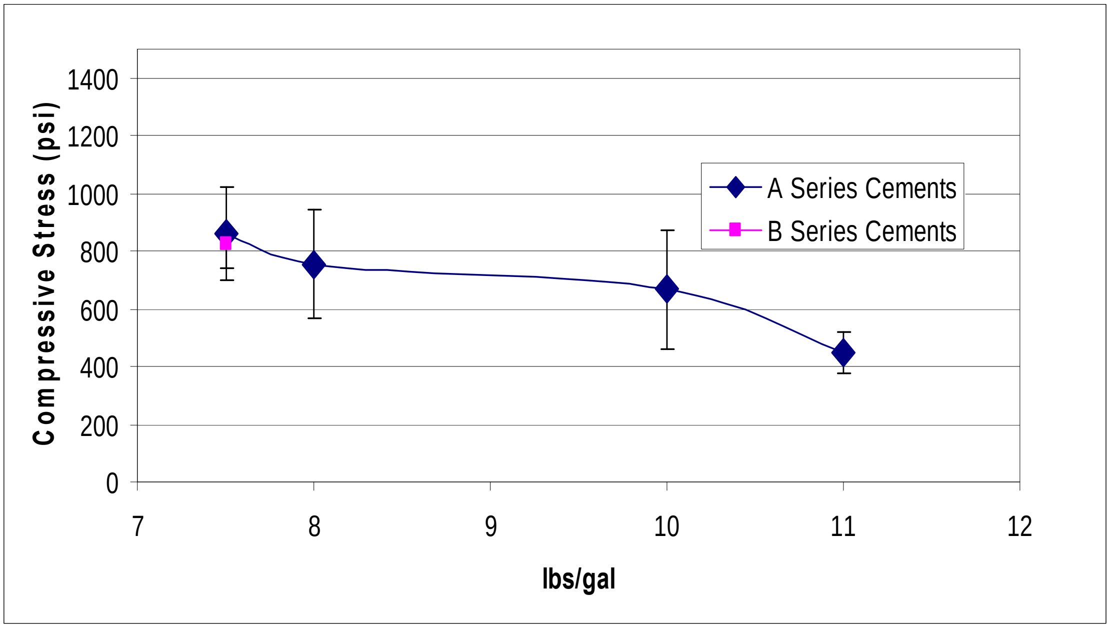

Figure 16. Compressive Strength of Cements as a function of MgO to Brine ratio. These A series cements were made with "impure" 33.2 ± 0.17% wgt $MgCl_2$ by weight brine and the B series cement was made with 'impure" 28.9±0.15% wgt $MgCl_2$. Error bars on the data points correspond to the standard deviation of 5 strength measurements.

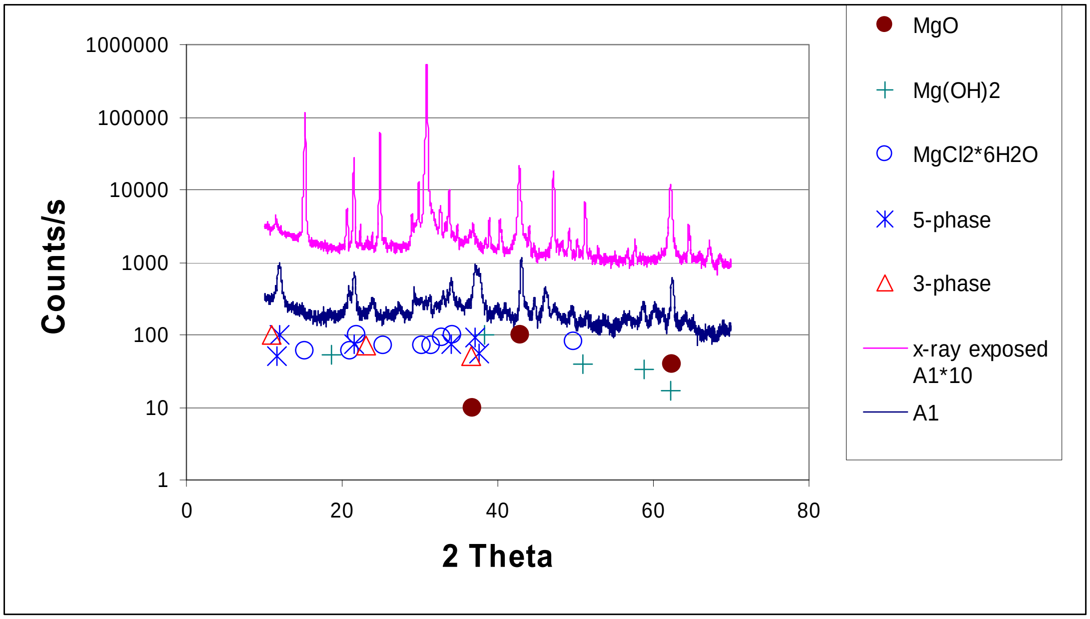

Figure 17. 24 hour x-ray spectra of Cement A1 corresponding to 0.8987 kg "crude" MgO per liter (7.5 lb "crude" MgO per gal) of "impure" 33.2±0.17% $MgCl_2$ brine when sample is exposed to x-rays for 24 Hrs and when it is not exposed to x-rays.

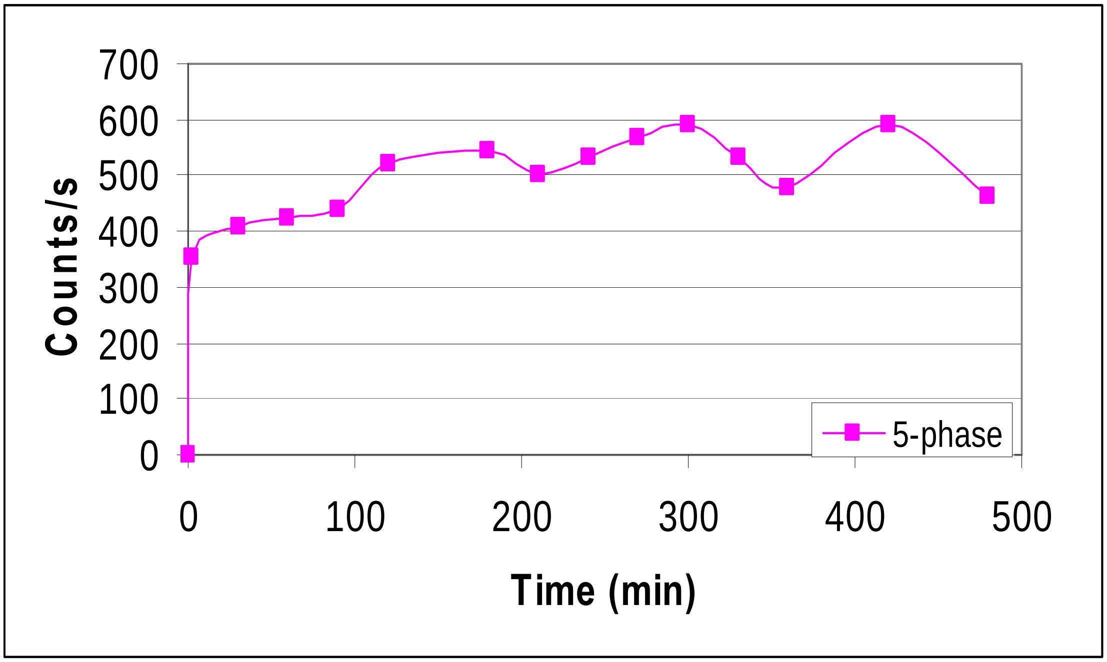

Figure 18. X-ray peak height for 5-phase (2θ= 11.9°) as a function of setting time.

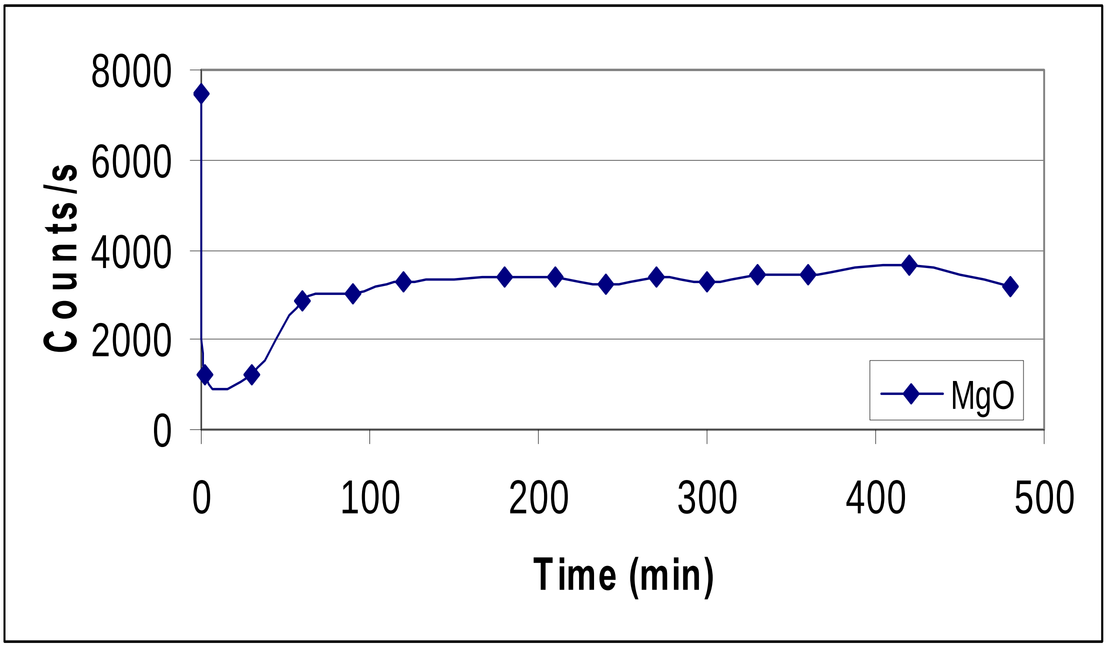

Figure 19. X-ray peak height for MgO phase (2θ= 42.9°) as a function of setting time for cement A1 0.8987 kg/L (7.5 lb/gal) 33.2±0.17% "impure" $MgCl_2$ brine.

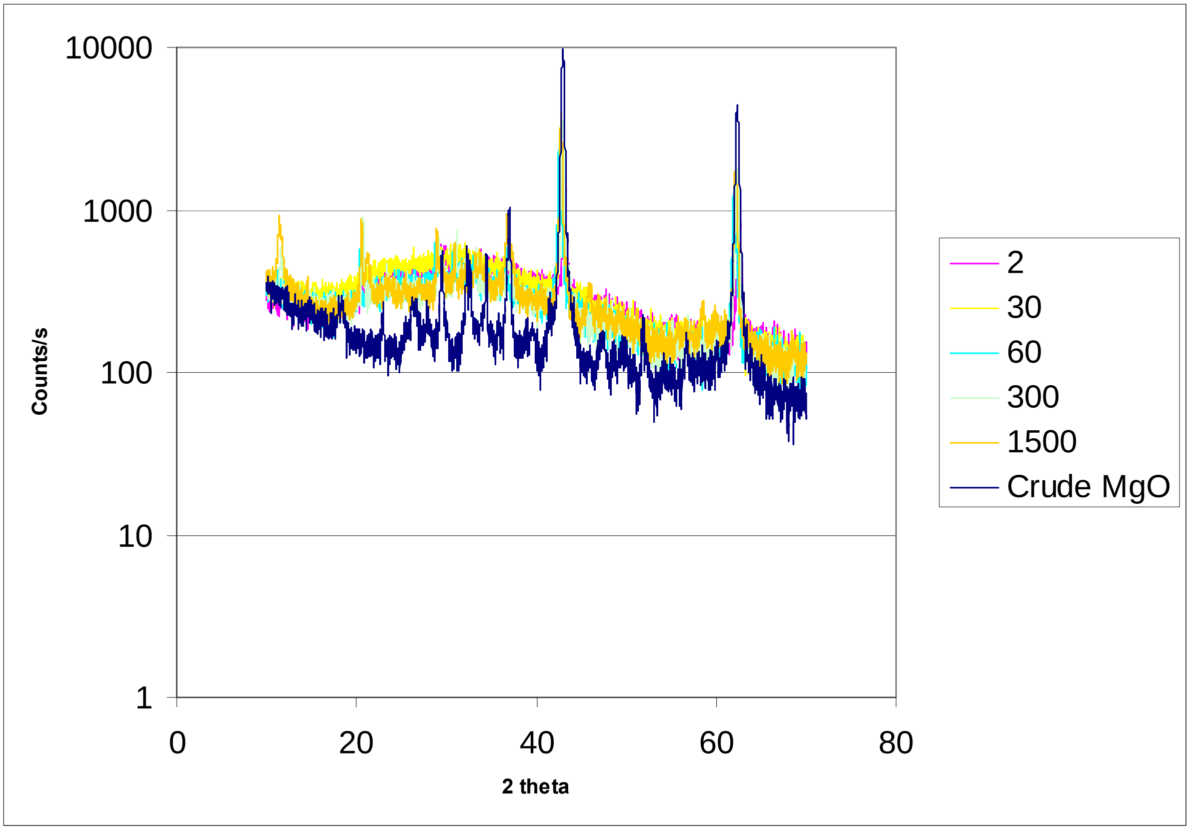

Figure 20. x-ray spectra as a function of setting time in minutes for Cement A1 corresponding to 0.8987 kg/L (7.5 lbs/gal) "crude" MgO in 33.2±0.17% "impure" $MgCl_2$.

9. TOC Graphic

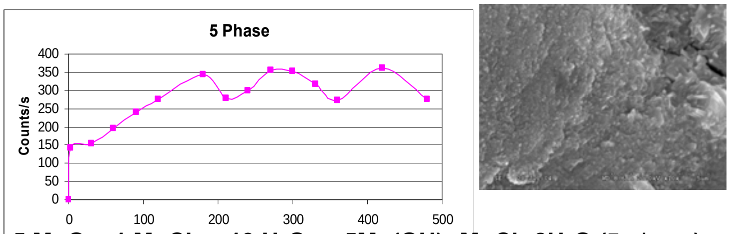

$5\,MgO + 1\,MgCl_2 + 13\,H_2O \rightarrow 5Mg(OH)_2\cdot MgCl_2\cdot 8H_2O$ (5-phase**)**

References

---

1 Matkovic, B., Popovic, S., Rogic, V., Zunic, T. and Young, J.F., J. Am. Ceramic Soc., 60(11-12) 504-507(1977).
2 Dehua, D. and Chuanmei, Z., Cement and Concrete Research 29,1365-1371(1999).
3 Zhang, Z-Y, Dai, C-L, Zhang, Q-H, Guo, B-Z and Liu, W-L., Science in China (Series B), 34(12)1501-1509(1991).
4 Dehua, D. and Chuanmei, Z., Cement and Concrete Research 29,1365-1371(1999).
5 Product Literature on MAGOX 98 HR, Premier Chemicals, LLC of Bettsville, OH.
6 Product specification sheet Great Salt Lake Minerals & Chemical Company, Salt Lake City, UT
7 Millipore Corporate Headquarters, 290 Concord Rd., Billerica, MA 01821, USA.
8 Hitachi Instruments Co. Ltd., Yotsuya 4-28-8 Shinjuku-ku, Tokyo 160-0004
9 Beckman Coulter, Inc., 4300 N. Harbor Boulevard, P.O. Box 3100, Fullerton, CA 92834-3100
10 PANalytical B.V. , Lelyweg 1, 7602 EA Almelo , The Netherlands
11 Instron Corporation Headquarters, 100 Royall Street, Canton, MA, 02021, USA
12 pHoenix Electrode Co., 6103 Glenmont, Huston, Texas 77081
13 Weast, R.C., “CRC Handbook of Chemistry and Physics,” 54th edition, CRC Press, Cleveland OH, 1974.
14 Hu, Yuerong; Liang, Jessica K.; Myerson, Allan S.; Taylor, Lynne S., *Industrial and Engineering Chemistry Research*, v 44, n 5, Mar 2, 2005, p 1233-1240.
15 Aber, Janice E.; Arnold, Stephen; Garetz, Bruce A.; Myerson, Allan S., *Physical Review Letters*, v 94, n 14, Apr 15, 2005, p 1-4.